

## **Kinetics and thermodynamics of the ferroelectric transitions in PbMg<sub>1/3</sub>Nb<sub>2/3</sub>O<sub>3</sub> and PbMg<sub>1/3</sub>Nb<sub>2/3</sub>O<sub>3</sub>-12% PbTiO<sub>3</sub> crystals**

Eugene V. Colla, Nathan Jurik, Yehan Liu, M. E. X. Delgado, M. B. Weissman, D. D. Viehland, and Z.-G. Ye

Citation: *Journal of Applied Physics* **113**, 184104 (2013); doi: 10.1063/1.4804069

View online: <http://dx.doi.org/10.1063/1.4804069>

View Table of Contents: <http://scitation.aip.org/content/aip/journal/jap/113/18?ver=pdfcov>

Published by the [AIP Publishing](#)

---

### **Articles you may be interested in**

[In-situ observation of domain wall motion in Pb\(In<sub>1/2</sub>Nb<sub>1/2</sub>\)O<sub>3</sub>-Pb\(Mg<sub>1/3</sub>Nb<sub>2/3</sub>\)O<sub>3</sub>-PbTiO<sub>3</sub> crystals](#)  
J. Appl. Phys. **116**, 034105 (2014); 10.1063/1.4890351

[Broadband inelastic light scattering study on relaxor ferroelectric Pb\(In<sub>1/2</sub>Nb<sub>1/2</sub>\)O<sub>3</sub>-Pb\(Mg<sub>1/3</sub>Nb<sub>2/3</sub>\)O<sub>3</sub>-PbTiO<sub>3</sub> single crystals](#)  
J. Appl. Phys. **115**, 234103 (2014); 10.1063/1.4878855

[Variations of composition and dielectric properties of Pb\(In<sub>1/2</sub>Nb<sub>1/2</sub>\)O<sub>3</sub>-Pb\(Mg<sub>1/3</sub>Nb<sub>2/3</sub>\)O<sub>3</sub>-PbTiO<sub>3</sub> single crystal along growth direction](#)  
J. Appl. Phys. **113**, 124105 (2013); 10.1063/1.4798287

[Ferroelastic aspects of relaxor ferroelectric behaviour in Pb\(In<sub>1/2</sub>Nb<sub>1/2</sub>\)O<sub>3</sub>-Pb\(Mg<sub>1/3</sub>Nb<sub>2/3</sub>\)O<sub>3</sub>-PbTiO<sub>3</sub> perovskite](#)  
J. Appl. Phys. **113**, 124102 (2013); 10.1063/1.4794027

[Structure, piezoelectric, and ferroelectric properties of BaZrO<sub>3</sub> substituted Bi\(Mg<sub>1/2</sub>Ti<sub>1/2</sub>\)O<sub>3</sub>-PbTiO<sub>3</sub> perovskite](#)  
J. Appl. Phys. **111**, 104118 (2012); 10.1063/1.4722286

---

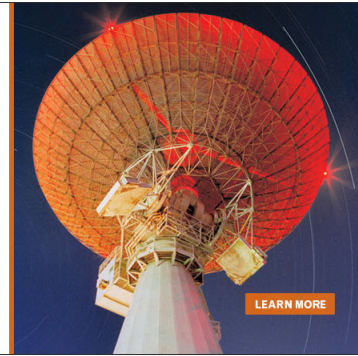
### MIT LINCOLN LABORATORY CAREERS

Discover the satisfaction of  
innovation and service  
to the nation

- Space Control
- Air & Missile Defense
- Communications Systems & Cyber Security
- Intelligence, Surveillance and Reconnaissance Systems

- Advanced Electronics
- Tactical Systems
- Homeland Protection
- Air Traffic Control

 **LINCOLN LABORATORY**  
MASSACHUSETTS INSTITUTE OF TECHNOLOGY



LEARN MORE

# Kinetics and thermodynamics of the ferroelectric transitions in $\text{PbMg}_{1/3}\text{Nb}_{2/3}\text{O}_3$ and $\text{PbMg}_{1/3}\text{Nb}_{2/3}\text{O}_3\text{-}12\%$ $\text{PbTiO}_3$ crystals

Eugene V. Colla,<sup>1</sup> Nathan Jurik,<sup>1</sup> Yehan Liu,<sup>1</sup> M. E. X. Delgado,<sup>1</sup> M. B. Weissman,<sup>1</sup> D. D. Viehland,<sup>2</sup> and Z.-G. Ye<sup>3</sup>

<sup>1</sup>Department of Physics, University of Illinois at Urbana-Champaign, 1110 West Green Street, Urbana, Illinois 61801-3080, USA

<sup>2</sup>Department of Materials Science and Engineering, Virginia Tech, 201 Holden Hall (0237), Blacksburg, Virginia 24061, USA

<sup>3</sup>Department of Chemistry and 4D Labs, Simon Fraser University, Burnaby, British Columbia V5A1S6, Canada

(Received 6 February 2013; accepted 22 April 2013; published online 10 May 2013)

The two-step freezing and melting of the field-induced ferroelectric order in  $\text{PbMg}_{1/3}\text{Nb}_{2/3}\text{O}_3$  (PMN) and  $(\text{PbMg}_{1/3}\text{Nb}_{2/3}\text{O}_3)_{0.88}(\text{PbTiO}_3)_{0.12}$  (PMN-PT) is investigated. In PMN-PT, direct microscopic images show that both steps occur in the same spatial regions. The higher temperature freezing corresponds to the higher temperature melting, indicating that the stages are not just kinetically but also thermodynamically distinct. The higher-T melting step shows several indications of being a sharp first-order transition near an equilibrium temperature. The lower-T melting step shows more kinetic dependence. Partially poled PMN also spontaneously approaches saturation polarization on zero-field aging, indicating that the true equilibrium state is ferroelectric below  $\sim 200$  K. In PMN-PT, a variety of kinetic measurements on the ferroelectric state indicate that the kinetics are governed by a glassy matrix showing aging effects. © 2013 AIP Publishing LLC. [http://dx.doi.org/10.1063/1.4804069]

## INTRODUCTION

The perovskite  $\text{PbMg}_{1/3}\text{Nb}_{2/3}\text{O}_3$  (PMN) is a canonical relaxor ferroelectric, as are solid solutions of  $\text{PbTiO}_3$  (PT) and PMN for low concentrations of PT (PMN-PT).<sup>1,2</sup> These relaxors show an electric-field-induced hysteretic first-order transition (actually a two-step transition; see, e.g., Ref. 3) into a partially disordered ferroelectric (FE) state.<sup>3–7</sup> Even in the FE state, a substantial fraction of the material can remain disordered, with FE nanoregions imbedded in a more disordered glassy matrix,<sup>8,9</sup> as expected theoretically for similar materials.<sup>10</sup>

In PMN-12%PT a FE state has been shown to be more stable than the unpolarized state below a transition temperature even when the electric field  $\mathbf{E}=0$ , but results on the phase stability in pure PMN were less definite.<sup>11</sup> Previous results on the two-step ordering transition found in those samples with relatively sharp transitions showed that the two steps involve substantially different ratios of changes in polarization and real and imaginary susceptibility, indicating that qualitatively different processes are involved in each step.<sup>3</sup> Those results, however, could not determine if the two steps are governed by different thermodynamic stabilities or by different kinetics.<sup>3</sup> Studies of detailed aging properties of the complex susceptibility show properties typical of spin-glass-like aging, not just domain growth, even in the FE state.<sup>12–14</sup>

In this paper we give results showing a thermodynamic rather than kinetic distinction between the two steps of the transition, setting some limits on the stability of the different FE phases, and showing that long-time kinetics of the FE order are strongly dependent on glassy correlations formed

in the absence of the FE order. We briefly discuss the indirect implications for pictures of the relaxor state and of the two steps of the ferroelectric transition.

Rough empirical phase diagrams of PMN and PMN-PT, as shown in Fig. 1, reveal several regimes. (By empirical phase diagram, we mean a picture of where the transitions and crossovers occur under typical lab conditions, leaving significant uncertainty as to where the true phase transition lines are for hysteretic transitions.) At high temperature, the material is an ergodic paraelectric (PE). Upon cooling at low  $|\mathbf{E}|$ , a rapid non-Arrhenius<sup>15</sup> crossover to a glassy relaxor state (RLX) occurs. In field-cooling (FC) at sufficient  $|\mathbf{E}|$  a transition to the FE state is found, with the transition being abrupt in some crystalline samples lacking visible defects.<sup>3–7</sup> The same transition can also be reached by applying  $\mathbf{E}$  after zero-field cooling (ZFC). Over a broad range of temperature ( $T$ ), reducing  $\mathbf{E}$  to zero leaves the material in a FE state. Thus, there is a broad hysteretic regime in which the thermodynamically stable state at low  $|\mathbf{E}|$  is not obvious from such simple characterizations.

Careful measurements of the formation of the FE phase show that in many samples, those in which the transition is sharpest, it occurs in two stages, detectable either as a function of time ( $t$ ) after applying  $\mathbf{E}$  after ZFC or as a function of  $T$  in a FC protocol.<sup>3</sup> In these same samples, it is generally found that the FE order melts in two stages on subsequent low- $|\mathbf{E}|$  warming. Two obvious limiting possibilities arise for this two-step transition. The first is that there are two different phase transitions with slightly different thermodynamic transition temperatures. The second is that the kinetics include a relatively fast step and a more sluggish one, perhaps involving the glassy degrees of freedom. In the

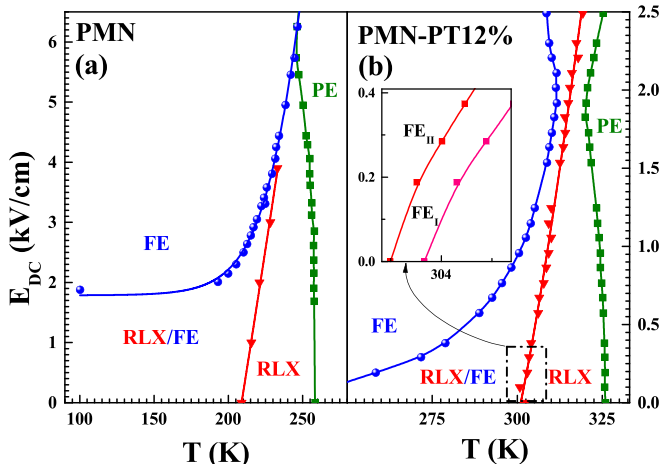


FIG. 1. Empirical phase diagrams for PMN and 12% PT. The PE to RLX line shows where the peak in the susceptibility occurs, marking the crossover from the PE state to the glassy relaxor (RLX). The RLX to RLX/FE line shows where FE order melts under slow heating. The FE to RLX/FE line shows where FE order forms under slow cooling. The inset for the second panel shows the positions of the two steps of the melting process.

thermodynamic case, the order formed first, in the higher-T freezing step, would melt second, in the higher-T melting step. In the kinetic case, the first order formed would also be the first to melt, so that the higher-T freezing would correspond to the lower-T melting. If (as we shall see) there are two thermodynamic phase transitions, the question raised above of sorting out the equilibrium phase diagram from the strongly hysteretic empirical phase diagram becomes more complicated, since there are now two transition lines to determine.

The broad hysteretic region is perhaps the most obvious of many symptoms of sluggish kinetics in the ferroelectricity of these materials. The glassy relaxor order, which does not entirely go away when the FE state is formed, is an obvious possible contributor to these slow kinetics. A variety of experiments on the effects of aging on the susceptibility<sup>12–14,16,17</sup> show behavior characteristic of spin-glasses, including the persistence of multiple “holes” in the susceptibility vs. T after aging at several T’s, unlike the effects of simple domain growth.<sup>18</sup> We show here that the kinetics of the formation and melting of FE states are indeed very sensitive to the history of the sample in the glassy, non-FE regime, even when the resulting FE states have virtually identical polarizations.

## MATERIALS AND METHODS

The PMN single crystals were grown from high temperature solution using PbO/B<sub>2</sub>O<sub>3</sub> as flux, according to the technique and the phase diagram described by Ye *et al.*<sup>19</sup> The samples of PMN-12%PT were grown by a modified Bridgman technique and provided by TRS Technologies (State College, PA). This concentration is well below the morphotropic phase boundary, above which all frozen phases are ferroelectric. Both samples were configured as parallel-plate capacitors oriented with the applied E along a [111] direction. The PMN sample was ~0.66 mm thick with ~3 mm<sup>2</sup> area and the PMN-PT sample was ~0.48 mm thick

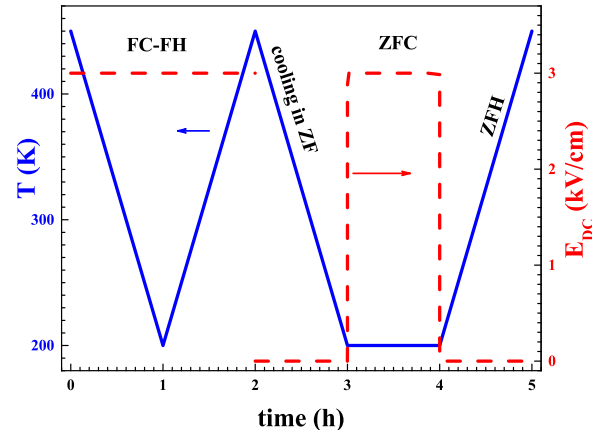


FIG. 2. Typical histories of T (solid line) and E (dashed line) for FC and ZFC protocols.

with ~1 mm<sup>2</sup> area. Contacts were made via evaporated Au layers of roughly 100 nm thickness on top of adhesion-enhancing ~10 nm thick Cr layers. The measurement circuitry used externally-fixed voltages on the sample and a current-sensing amplifier. The near-dc polarization current and ac current response to applied ac voltages could be measured simultaneously.

To form the field-induced ferroelectric state the samples were either cooled in an applied E-field or cooled in E = 0, with the field subsequently applied at low T. Then, after varying durations of aging with |E| > 0, we set E = 0 and measured the kinetics of melting via the depolarization current found on warming. Figure 2 shows the profile of T vs. time (t) for examples of the FC and ZFC protocols.

## DETAILED PROTOCOLS AND RESULTS

Our first step was to check that the two stages often seen in the transition between FE and PE in visually homogeneous samples did indeed occur in the same overall geometrical regions, as previously inferred,<sup>3</sup> rather than in isolated regions. This was done by direct optical imaging with a polarized-light microscope, as shown in Fig. 3. The PMN-PT sample was driven to polarize with a field of 3.13 kV/cm at T = 280 K. The changes evident in the still photographs occur primarily in two distinct steps, unmistakably evident to an untrained eye in the moving-picture images, available in the supplementary material.<sup>20</sup> After gradual initial formation of polarized regions near the electrodes, the main region becomes partially polarized in a rapid step. Then after some slow creep of boundary regions, the main region very rapidly switches to more complete polarization. Each rapid step covers essentially the whole region in which the field is applied. These optical images do not resolve, however, whether the two steps involve different regions on the few-nanometer scale<sup>8–10</sup> of the intrinsic relaxor heterogeneity.

Fig. 4 illustrates the two-step polarization-depolarization process for both samples under a variety of protocols described in the captions. The sharpness of the separation between the steps is somewhat dependent on the protocol.

By reversing the temperature sweep just after the first polarization step, we could check which depolarization step

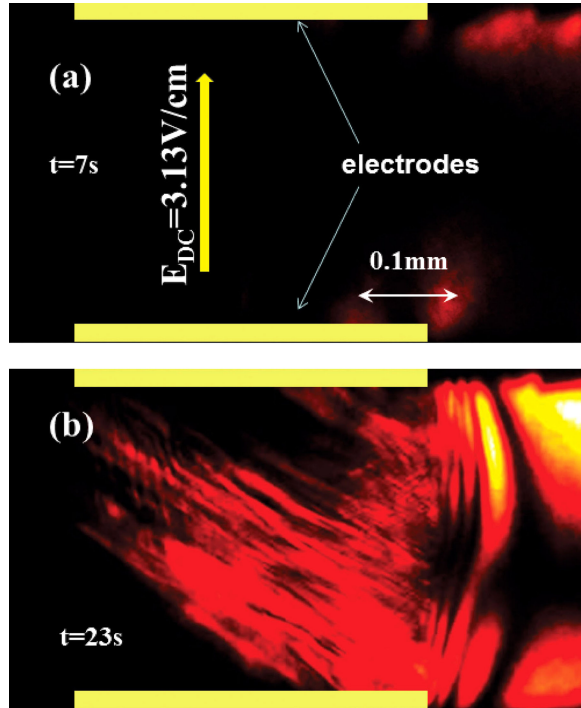


FIG. 3. Polarized-light pictures of the PMN-PT sample before (a) and after (b) polarization in a field (enhanced in supplementary material).

corresponds to which polarization step,<sup>21</sup> as shown in Fig. 5. Clearly the initial high-temperature step on cooling corresponds to the second, also high-temperature, step on warming.<sup>21</sup> Thus in PMN the two steps appear to be distinguished thermodynamically, and not primarily by different kinetics.

In PMN-PT the polarization shows two easily resolved steps under high fields ( $\sim 1.3\text{ kV/cm}$ ) especially at low cooling rates (e.g., 0.2 K/min). However, the two peaks are not

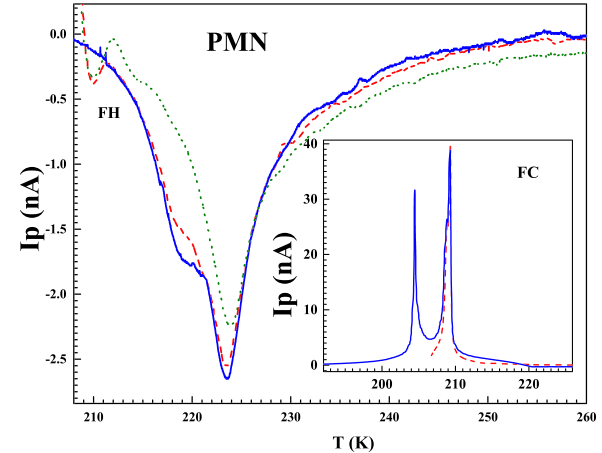


FIG. 5. The depolarization  $I_p(t)$  for PMN is shown on warming after polarization in a field of  $2.13\text{ kV/cm}$ . The solid curve shows depolarization after cooling to  $140\text{ K}$  and then warming. The lower depolarization step is present here as a distinct shoulder. When the polarization is interrupted after one step (shown in the dashed line in inset) by only cooling to  $205\text{ K}$  and then immediately reheating (the dotted curve) the lower depolarization step is missing. The dashed line represents the same protocol as the dotted line but with the partially polarized sample was aged in field for  $10\text{ min}$  at  $205\text{ K}$ . All temperature sweeps were at  $4\text{ K/min}$ .

well resolved on cooling at lower fields and higher rates. The steps are easily resolved when the polarization is formed slowly after a ZFC protocol, as is clear in Fig. 4(c).

Fig. 6 illustrates that in PMN-PT, as in PMN, the high-temperature freezing peak corresponds to the high-temperature melting peak. In the  $I_p(t)$  plots shown, the high- $T$  peak appears as sharp spikes on FC cooling and ZFC warming, unlike the broader lower- $T$  processes. When the FC cooling is interrupted after the first freezing step, only the sharp spike remains on warming. This result was checked

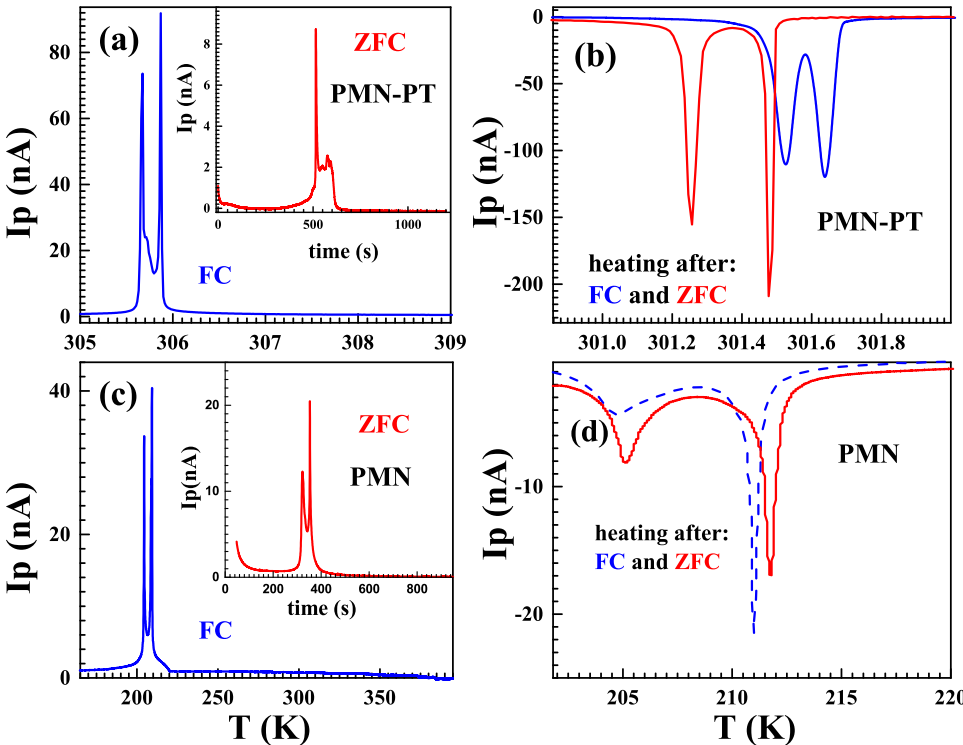


FIG. 4. The two-stage polarization-depolarization current is shown for both samples and several protocols. (a) PMN-PT on cooling at  $4\text{ K/min}$  in a field of  $1.12\text{ kV/cm}$ . Inset:  $I_p$  vs.  $t$  after setting  $E = 0.48\text{ kV/cm}$  after ZFC to  $280\text{ K}$ . (b) PMN-PT on warming at  $4\text{ K/min}$  in  $E = 0$ . (c) PMN on cooling at  $4\text{ K/min}$  in a field of  $2.43\text{ kV/cm}$ . Inset:  $I_p$  vs.  $t$  after setting  $E = 2.43\text{ kV/cm}$  after ZFC to  $200\text{ K}$ . (d) PMN on warming at  $4\text{ K/min}$  in  $E = 0$ .

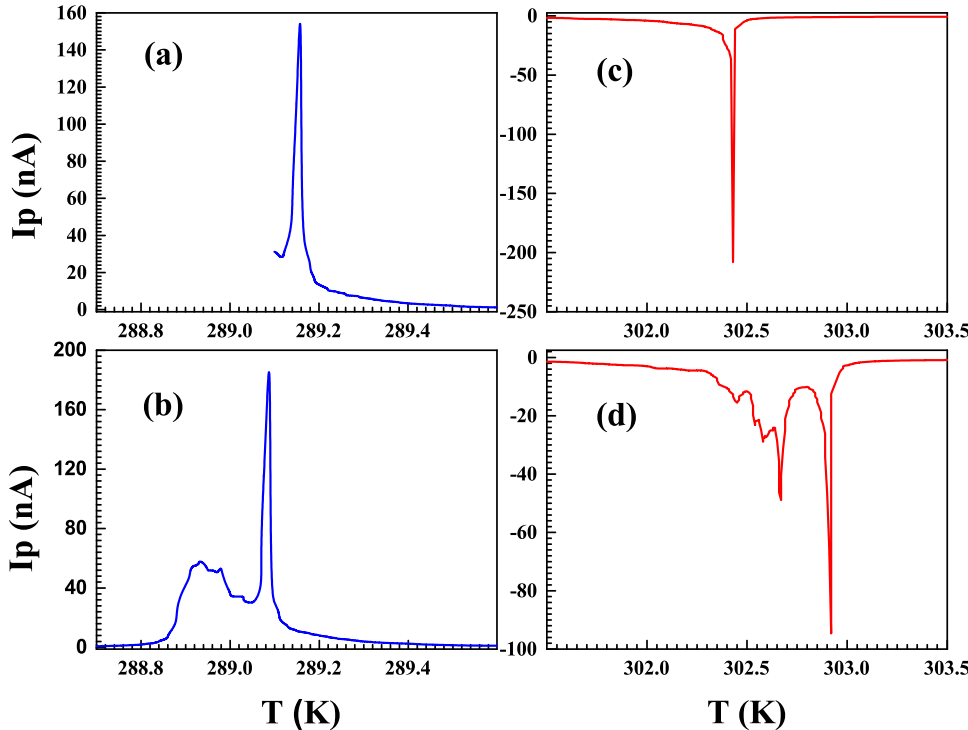


FIG. 6.  $I_p$  is shown for PMN-PT for (a) an interrupted cooling at 4 K/min and  $E = 0.56 \text{ kV/cm}$ . (b) An uninterrupted cooling showing both freezing stages. (c) Melting on warming at 4 K/min after interrupted freezing. (d) Melting after complete freezing. The slight shift of the peak temperature on melting is characteristic of different aging times in the frozen state.

by also tracking  $\epsilon''$ , which shows a distinct peak only at the higher-T steps, with the peak remaining on warming after interrupted freezing.

It thus appears that in these materials there are two thermodynamic transitions, reflecting two types of order with slightly different stability. Henceforth we shall refer to two types of FE order,  $\text{FE}_I$  and  $\text{FE}_{II}$ , to distinguish the polarization corresponding to the higher T and lower T steps, respectively.

The next question to address is the thermodynamic stability of the FE states within the hysteretic regime, in particular whether either is ever stable at  $E = 0$ . Consistent with prior results,<sup>11</sup> the PMN-PT sample spontaneously reaches nearly complete polarization once it has been given a bit of initial polarization to break inversion symmetry. Thus in most of the hysteretic region in PMN-PT the fully polarized state ( $\text{FE}_{II}$ ) is more stable than the unpolarized states and is, most likely, the thermodynamic ground state. This means that in the equilibrium phase diagram, both lines representing the two-step conversion to  $\text{FE}_{II}$  must intersect the  $E = 0$  axis not far below the empirical melting temperature, although the slow kinetics make it hard to measure the precise temperatures of those two equilibrium transitions.

In PMN, the result is similar though less clear-cut.<sup>21</sup> Fig. 7 shows the depolarization currents after different times of zero field aging at 200 K. The lower-T depolarization peak is almost entirely lost for aging time of 10 h. Below  $\sim 196$  K, it is preserved. In fact, below 196 K we find no condition under which the samples spontaneously lose polarization at  $E = 0$ , but we do find that if the sample is substantially polarized, it will spontaneously approach full polarization even at  $E = 0$ .<sup>21</sup> At  $E = 0$  all aging above  $\sim 200$  K leads to loss of polarization. The most plausible interpretation is that the  $\text{FE}_{II}$  state is the equilibrium state in

the lower-T range and the depolarized relaxor is the equilibrium state in the higher-T range. There is probably an intermediate equilibrium  $\text{FE}_I$  state in the narrow range near 200 K, since the  $\text{FE}_{II}$  polarization is lost but the melting temperature of the  $\text{FE}_I$  state increases on aging in that range.

The extent of polarization of the FC and ZFC states can be compared using the integral of the depolarization currents. Within the error bars ( $\sim 10\%$ ) the polarizations are equal. Nevertheless the ZFC and FC states are not the same, as can be seen in the kinetic measurements. Fig. 8 shows the time before the abrupt depolarization occurs as a function of the temperature at which zero-field warming is halted in PMN-PT. This depolarization time shows approximately activated behavior, with a larger activation energy after the ZFC polarization protocol than after the FC protocol.

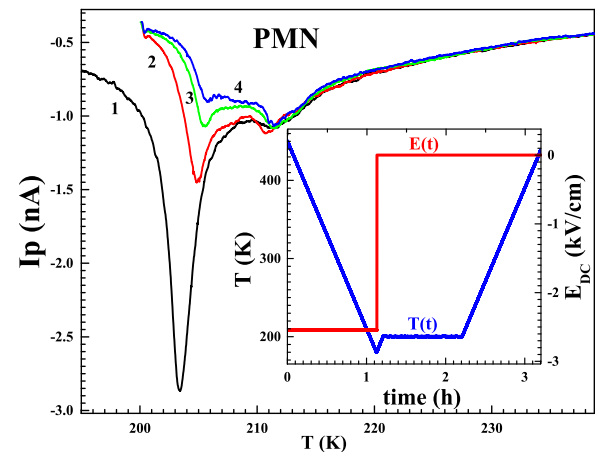


FIG. 7. Depolarization currents after field cooling in  $2.55 \text{ kV/cm}$  of the PMN sample, then ZF aging at 200 K for  $t = 0$  (1), 1 h (2), 4 h (3), 10 h (4). The insert shows the protocol of the experiment.

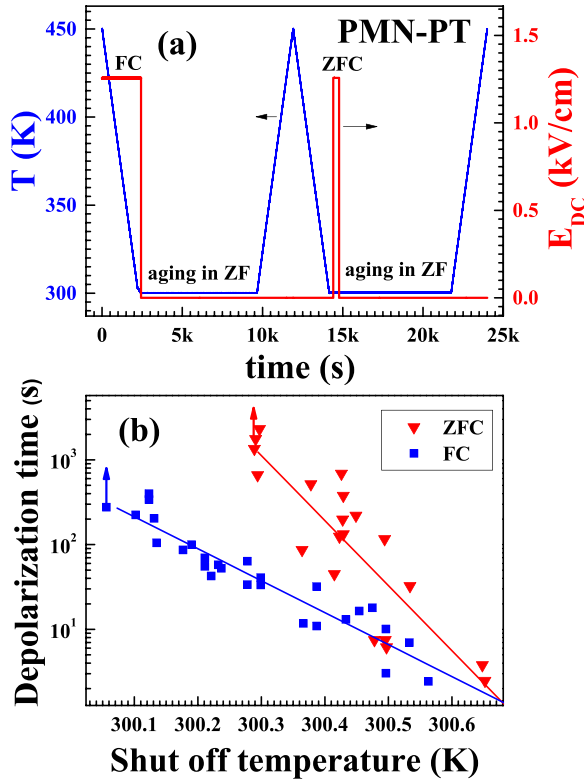


FIG. 8. The times required for the abrupt depolarization to occur on sitting at  $E=0$  as a function of  $T$ , after warming a ZFC and a FC polarized PMN-PT sample from 300 K. The sample was polarized in  $E=1.25$  kV/cm via a FC or a 300 K ZFC protocol before aging at  $T=300$  K and  $E=0$  until it lost the polarization. Below the temperatures marked by arrows the polarization is stable.

Likewise, a plot (Fig. 9) of PMN-PT depolarization magnitude after aging for 120 min at a range of temperatures shows that the ZFC state depolarizes more slowly.

The obvious question is what aspect of these equally polarized materials differs enough to make such major kinetic effects. Since the domains in the FC material initially form under the influence of  $\mathbf{E}$ , at a slightly higher  $T$  than for the ZFC material, one might expect that there would be

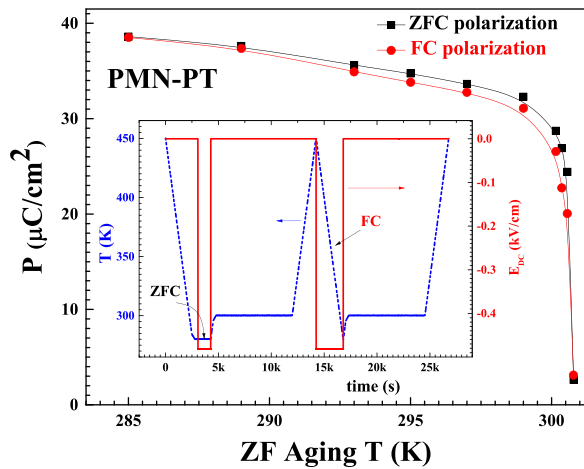


FIG. 9. Post-aging polarization is shown for two different polarization protocols as a function of temperature at which the sample is subsequently aged at ZF for 120 min. The polarization protocols, shown in the inset, both involve the same field and cooling to 280 K, in one case in field and in the other in cooling in zero field.

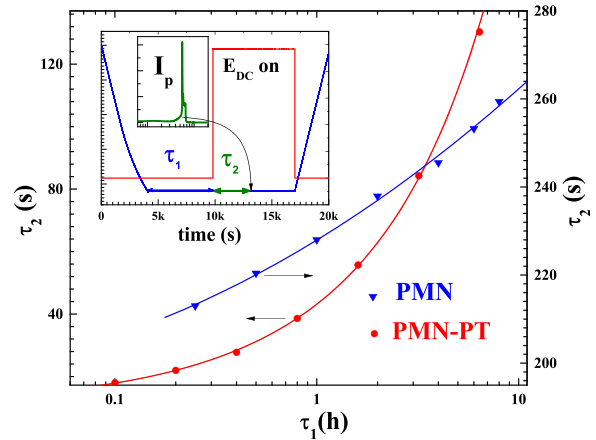


FIG. 10. The time  $\tau_2$  to field-polarize the samples as a function of time  $\tau_1$  of prior aging at  $T$  but with  $E=0$ . The PMN-PT sample was held at 280 K under  $E=480$  V/cm, the PMN at 195 K and  $E=2.5$  kV/cm. The inset shows the form of the T-E protocol.

fewer domain walls and slower kinetics in the FC than in the ZFC material. The opposite is found, providing an initial indication that the kinetics are governed by glassy degrees of freedom, as had been previously surmised.<sup>14</sup>

Fig. 10 shows the dependence of the time to field-polarize the PMN-PT and PMN samples in the ZFC regime as a function of prior time aged at the same  $T$  but with  $E=0$ . There is a dramatic decrease in rates as a function of aging time. Since the aging is done in the glassy state, it is more plausible to attribute it to the growth of glassy correlations than to any FE domain process, since if FE domain growth initiated at  $E=0$  one would expect that to speed rather than slow the formation of longer-range FE order.

Fig. 11 shows the dependence on aging time (at 300.4 K under  $E=1.25$  kV/cm) of the time required for the abrupt depolarization to occur after warming a ZFC PMN-PT sample to 300.4 K. It is evident that under aging in field the FE state here continues to stabilize. Stabilization of the FE state under aging would be compatible with either the gradual growth of FE domains or the gradual equilibration of the detailed state of the glassy regions between domains with the

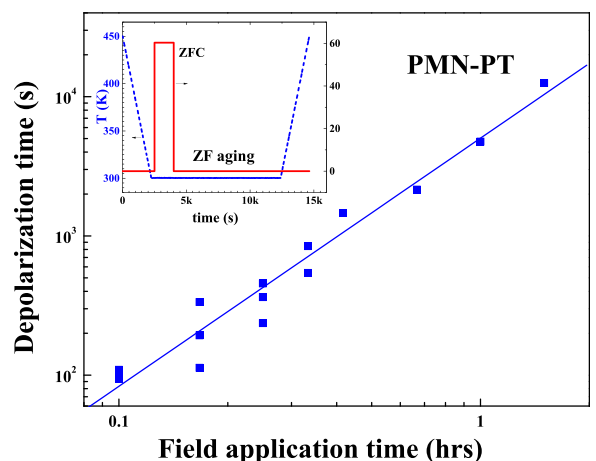


FIG. 11. The time required for the abrupt depolarization to occur on sitting at  $E=0$  and  $T=300.4$  K after warming a ZFC polarized sample as a function of time spent at  $E=1.25$  kV/cm at  $T=300.4$  K.

domains, e.g., via adjustment to the non-uniform strain produced by the non-cubic domains. The time to depolarize grows more than linearly with the aging time, for which the only apparent explanation is that the energy barriers are growing. Together with the other aging results, that would best fit the second explanation, based on gradual adjustment of the glassy regions.

## DISCUSSION

Key features of the equilibrium phase-diagram of PMN and its low-PT solid solutions are now clearer. There are *two* FE states with similar but not identical transition temperatures. At least the higher-T one of these states is stable at  $E=0$  in both PMN and PMN-12%PT below a temperature close to the standard empirical melting temperature. The lower-T FE state is also stable at slightly lower temperature at  $E=0$  in PMN-12%PT. Our data do not currently suffice to prove that this lower transition line crosses  $E=0$  in PMN, because the kinetics become inaccessibly slow in the region where this transition is expected at  $E=0$ .

From the slope in the E-T plane of the FE melting lines, which are close to the true phase transition line, one can infer an approximate entropy loss on formation of the FE phase,  $S$ . The change in free energy per unit cell as a function of  $E$  is simply determined by the known polarization of the FE phase ( $P \sim 30 \mu\text{C}/\text{cm}^2$ ). PdE must balance  $SdT/V_U$  along the equilibrium line. For both samples we obtain roughly  $S/V_U = 0.04 \text{ k}_B$ , where  $\text{k}_B$  is Boltzmann's constant. The low dimensionless entropy per unit cell is a reminder that the units which align to form the FE phase are primarily nanodomains consisting of many unit cells. In addition, any local polarizations which may align within or between nanodomains would also be largely aligned in the glassy phase, and thus have low entropy despite its lack of a simple order parameter.

Even when the material is close to the nominal saturation polarization, the disordered degrees of freedom continue to govern the slow kinetics of the forming and melting of the FE state, just as they govern the detailed ac susceptibility.<sup>12–14,16,17,22</sup> Aging at  $E=0$ , with no evidence that any FE domains are present above the scale of the nanodomains, leads to dramatic slowing of these kinetics.

## PROSPECTS AND IMPLICATIONS

At least one obvious question remains open: What are the structures of the two ferroelectric states? Does the symmetry breaking from cubic to rhombohedral occur in two steps, via an intermediate symmetry? Does the whole symmetry breaking occur in one step, but with the glassy regions only joining the ordered state in a second step? These obvious scenarios do not exhaust the possibilities. X-ray or neutron scattering would be the techniques of choice to resolve this question. Given that we have shown that long-time stable versions of either state can be reliably and reproducibly produced by suitable field-temperature protocols, such experiments are entirely feasible.

These results have some relevance to the characterization of the glassy relaxor state. It has been argued that in

some regards it resembles a Griffiths phase, dominated by clusters of an incipient ordered phase, with the Burns temperature corresponding to the Griffiths temperature.<sup>23,24</sup> The existence of a thermodynamic ordered ferroelectric phase even in pure PMN at  $E=0$  is consistent with that general approach. The persistence of effects of glassy kinetics even in the ferroelectric phase, however, is a reminder that, unlike in the simplest Griffiths pictures, other types of order are competing with the ferroelectric order, so that at low temperature the clusters do not simply link up to form the ordered state. At a minimum, there are the well-known strong quenched random fields, absent in magnetic Griffiths phases due to time-reversal symmetry. In addition, even within the ordered regions there appear to be some glassy displacements orthogonal to the FE polarization.<sup>8</sup> The combination of Griffiths-like cluster effects, vector random fields, and glassy displacements orthogonal to the main order, as in re-entrant spinglasses,<sup>25</sup> makes relaxor physics particularly complicated.

## ACKNOWLEDGMENTS

This work was funded by NSF DMR 02-40644 and used facilities of the Center for Microanalysis of Materials, University of Illinois, which is partially supported by the U.S. Department of Energy under Grant No. DEFG02-91-ER4543.

- <sup>1</sup>G. A. Smolenskii, V. A. Isupov, A. I. Agronovskaya, and Y. V. Popov, Sov. Phys. Solid State **2**, 2584–2594 (1961).
- <sup>2</sup>L. E. Cross, *Ferroelectrics* **151**, 305–320 (1994).
- <sup>3</sup>E. V. Colla and M. B. Weissman, *Phys. Rev. B* **72**, 104106-1–7 (2005).
- <sup>4</sup>G. Schmidt, H. Arndt, J. V. Cieminski, T. Petzsche, H.-J. Voigt, N. N. Krainik, *Kristall und Technik* **15**, 1415–1421 (1980).
- <sup>5</sup>G. Schmidt, H. Arndt, G. Borchhardt, J. v. Cieminski, T. Petzsche, K. Borman, A. Sterenberg, A. Zirmite, and V. A. Isupov, *Phys. Status Solidi A* **63**, 501–510 (1981).
- <sup>6</sup>E. V. Colla, E. Y. Koroleva, N. M. Okuneva, and S. B. Vakhrushev, *Ferroelectrics* **184**, 209–215 (1996).
- <sup>7</sup>B. Dkhil and J. M. Kiat, *J. Appl. Phys.* **90**, 4676–4681 (2001).
- <sup>8</sup>I. K. Jeong, T. W. Darling, J. K. Lee, T. Proffen, R. H. Heffner, J. S. Park, K. S. Hong, W. Dmowski, and T. Egami, *Phys. Rev. Lett.* **94**, 147602-4 (2005).
- <sup>9</sup>R. Blinc, V. Laguta, and B. Zalar, *Phys. Rev. Lett.* **91**, 247601-1–4 (2003).
- <sup>10</sup>B. P. Burton, E. Cockayne, and U. V. Waghmare, *Phys. Rev. B* **72**, 064113-1–5 (2005).
- <sup>11</sup>E. V. Colla, D. Vigil, J. Timmerwilke, M. B. Weissman, D. D. Viehland, and B. Dkhil, *Phys. Rev. B* **75**, 214201-1–6 (2007).
- <sup>12</sup>L. K. Chao, E. V. Colla, and M. B. Weissman, *Phys. Rev. B* **74**, 014105-1–8 (2006).
- <sup>13</sup>E. V. Colla, M. B. Weissman, P. M. Gehring, G. Xu, H. Luo, P. Gemeiner, and B. Dkhil, *Phys. Rev. B* **75**, 024103-1–5 (2007).
- <sup>14</sup>E. V. Colla, P. Griffin, M. Delgado, M. B. Weissman, X. Long, and Z.-G. Ye, *Phys. Rev. B* **78**, 054103-1–5 (2008).
- <sup>15</sup>A. E. Glazounov and A. K. Tagantsev, *Appl. Phys. Lett.* **73**, 856–858 (1998).
- <sup>16</sup>E. V. Colla, L. K. Chao, M. B. Weissman, and D. D. Viehland, *Phys. Rev. Lett.* **85**, 3033–3036 (2000).
- <sup>17</sup>E. V. Colla, L. K. Chao, and M. B. Weissman, *Phys. Rev. B* **63**, 134107-1–10 (2001).
- <sup>18</sup>E. Vincent, V. Dupuis, M. Alba, J. Hammann, and J.-P. Bouchaud, *Europhys. Lett.* **50**, 674–680 (2000).
- <sup>19</sup>Z.-G. Ye, P. Tissot, and H. Schmid, *Mater. Res. Bull.* **25**, 739 (1990).
- <sup>20</sup>See supplementary material at <http://dx.doi.org/10.1063/1.4804069> for a movie showing optical polarization of the sample as it undergoes a two-step ferroelectric transition.
- <sup>21</sup>M. Delgado, “The Freezing Mechanisms of Perovskite Relaxor Ferroelectrics and the Thermodynamic Stability of Their Ferroelectric

- States” M.S. Thesis, University of Illinois at Urbana-Champaign, 2009.
- <sup>22</sup> M. B. Weissman, E. V. Colla, and L. K. Chao, *AIP Confer. Proc.* **677**, 33 (2003).
- <sup>23</sup> B. P. Burton, E. Cockayne, S. Tinte, and U. V. Waghmare, *Phys. Rev. B* **77**, 144114-1-8 (2008).
- <sup>24</sup> V. A. Stephanovich, *Eur. Phys. J. B* **18**, 17–21 (2000).
- <sup>25</sup> J. M. D. Coey, *Can. J. Phys.* **65**, 1210–1232 (1987).